GA-A--20959

DE92 018885

A MODEL FOR ANALYTICAL PERFORMANCE PREDICTION OF HYPERVAPOTRON

by
C.B. BAXI and H. FALTER*

This is a preprint of a paper to be presented at the Fifth International Topical Meeting on Nuclear Reactor Thermal Hydraulics (NURETH-5), September 21–24, 1992, Salt Lake City, Utah, and to be printed in the *Proceedings*.

Work supported by
U.S. Department of Energy
Contract No. DE-AC03-89ER51114

* JET Joint Undertaking, Abingdon, Oxfordshire, England

GENERAL ATOMICS PROJECT 3467
JULY 1992

GENERAL ATOMICS

A MODEL FOR ANALYTICAL PERFORMANCE PREDICTION OF HYPERVAPOTRON

C.B. Baxi, *General Atomics*
P.O. Box 86508
San Diego, California 92138-5608, U.S.A.
(619) 455-3150; FAX (619) 455-2266

H. Falter, *JET Joint Undertaking*
Abingdon, Oxfordshire
OX14 3EA, England
(0235) 464473; FAX (0235) 464838

ABSTRACT. A hypervapotron is a water-cooled device which combines the advantages of finned surfaces with the large heat transfer rates possible during boiling heat transfer. Hypervapotrons have been used as beam dumps in the past and plans are under way to use them for divertor cooling in the Joint European Torus (JET). Experiments at JET have shows that a surface heat flux of 25 MW/m^2 can be achieved in hypervapotrons. This performance makes such a device very attractive for cooling of divertor of the International Thermonuclear Experimental Reactor (ITER). This paper presents an analytical method to predict the thermal performance of the hypervapotrons. Preliminary results show an excellent agreement between experimental results and analytical prediction over a wide range of flow velocities, pressures, subcooling temperatures and heat fluxes. This paper also presents the predicted performance of hypervapotron made of materials other than copper. After further development and verification, the analytical method could be used for optimizing designs and performance prediction.

I. INTRODUCTION

A hypervapotron consists of a finned surface made of high conductivity material such as copper (Fig. 1). The coolant is subcooled water at a high velocity and high pressure that flows perpendicular to the fins. Miller[1] has discussed the types of possible flows in such a geometry. Experiments by Falter et al.[2,3] have shown that the ideal geometry consists of fins with a height to pitch ratio of about 0.5. A recent paper by Greiner[4] discusses resonant heat transfer in a geometry similar to hypervapotron. However, this study is limited to laminar forced convection flow.

Hypervapotrons have been used at JET as beam dumps to remove large heat fluxes under steady-state conditions. Now plans are under way to install these with beryllium tiles brazed to the front surface as divertor targets. Extensive experiments have been carried out on hypervapotrons at the 10 MW JET Neutral Beam Test Bed.[2,3] The test parameters cover a wide range of geometry, pressure, velocity and subcooling. Peak surface heat fluxes of about 25 MW/m^2 have been obtained in these tests.

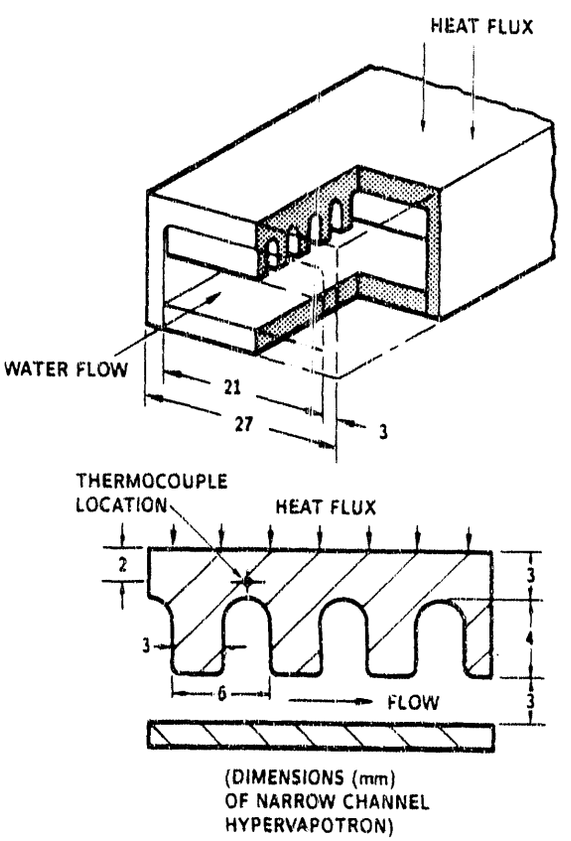

Fig. 1. Hypervapotron geometry. Dimensions are in millimeters (typical fin height = 3–6 mm, thickness = 3 mm, pitch = 6 mm).

At low heat fluxes the heat transfer is by forced convection. As the heat flux is increased, some of the surface reaches the incipient boiling temperature of the coolant. With further increase in heat flux, critical heat flux conditions will be reached on part of the heat transfer surface. Ultimately, part of the surface will melt. The experiments were never extended to this range. The maximum temperature is a function of water pressure, hypervapotron geometry, velocity of flow, length of hypervapotron, heat flux and coolant inlet temperature.

In this paper, an attempt is made to predict the thermal performance of hypervapotrons by a combination of heat transfer correlations and finite element analyses. If such an analytical prediction is feasible, designs could be optimized and performance predicted for untested conditions, materials and geometries.

II. DESCRIPTION OF THE EXPERIMENT

The experiments referred to in this paper were performed by Falter and his colleagues[2,3] in the JET Neutral Injection Test Bed. The hypervapotron tested had the external dimensions

Width:	75 mm
Height:	19 mm
Beam Exposed Length:	175 mm

The thermocouples used to measure the temperatures were located 2 mm below the high heat flux surface (Fig. 1). The surface temperature could be extrapolated from this measurement. Comparison with IR camera readings indicated that such an extrapolation was valid. The temperatures were measured at the center (axially) of the heated length.

III. ANALYSIS

A. Heat Transfer Correlations

The heat transfer is in three different regions. The units of the parameters are given in the nomenclature.

1. Forced convection: The following Modified Dittus Boelter correlation[5] was used for temperatures less than incipient boiling temperature.

$$Nu = 0.023\ (ff)\ \ (Re)^{0.8}\ \ (Pr)^{0.33} \quad . \qquad (1)$$

The factor $ff = 1.35$ is used to account for the re-circulating flow which occurs in the channels formed by the fins.[1] This factor was obtained by comparing calculated results with measured results[2,3] at a variety of flow velocities and geometries at low heat fluxes. The hydraulic diameter used in Re and Nu was the hydraulic diameter of the flow channel without fins.

2. Transition from forced convection to Nucleate boiling. The incipient boiling temperature is at the intersection of Eq. (1) and the Bergles Rosenow correlation.[6]

$$q'' = 1.8\ E - 3\,(p)^{1.156}\ \ (1.8\,\Delta T_{\rm SAT})^{2.8/(p)^{0.0234}}_{\rm ONB} \quad . \qquad (2)$$

3. Nucleate boiling. The nucleate boiling heat flux was calculated by Thom's correlation[7]:

$$q''_{\rm B} = 10^6\ \left[e^{p/87E5}\,(T_{\rm W} - T_{\rm SAT})\,/22.65\right]^2 \quad . \qquad (3)$$

The heat flux for temperatures greater than the incipient boiling temperature was calculated by[8]

$$\frac{q''}{q''_{\rm FC}} = \left[1 + \frac{(q''_{\rm B})^2}{(q''_{\rm FC})^2}\left(1 - \frac{q''_{\rm BI}}{q''_{\rm B}}\right)^2\right]^{1/2} \quad , \qquad (4)$$

where $q''_{\rm BI} = q''_{\rm B}$ at $T_{\rm ONB}$. This procedure is similar to the procedure shown in Fig. 5.10 of Ref. 9.

4. Critical heat flux was calculated by the MacBeth correlation.[9-12]

$$\left(q''_{\rm CRIT} \times 10^{-6}\right) = \frac{A + D(G \times 10^{-6})\,(\Delta i_{\rm sub})_{\rm i}}{C + z} \quad , (5)$$

where

$$A = y_0\, D^{y_1}\ \left(G \times 10^{-6}\right)^{y_2} \quad , \qquad (6)$$

$$C = y_3\, D^{y_4}\ \left(G \times 10^{-6}\right)^{y_5} \quad . \qquad (7)$$

The constants are listed in Ref. 9. This particular correlation was chosen because it takes into consideration effect of geometry and pressure. It is applicable at relatively low pressures and high velocities in the hypervapotron.

It was assumed that beyond the critical heat flux value calculated by Eq. (5), the heat flux remained constant with further increase in surface temperature. This gave good agreement between experiment and theory.

All above correlations require calculation of the heat flux as a function of local surface temperature for each set of conditions (geometry, pressure, coolant bulk temperature, and flow rate). Hence, all above equations were programmed in a computer code which created the input for the finite element code TOPAZ2D.[13]

The local heat transfer coefficient was calculated as

$$h = \frac{q''}{(T_s - T_B)} \quad , \tag{8}$$

where q'' = heat flux at a surface temperature T_s calculated by above procedure,

T_s = local surface temperature,

T_B = bulk temperature of the coolant at the calculation section.

Figure 2 shows a typical variation of the heat transfer coefficient as a function of local surface temperature in the cooling channel.

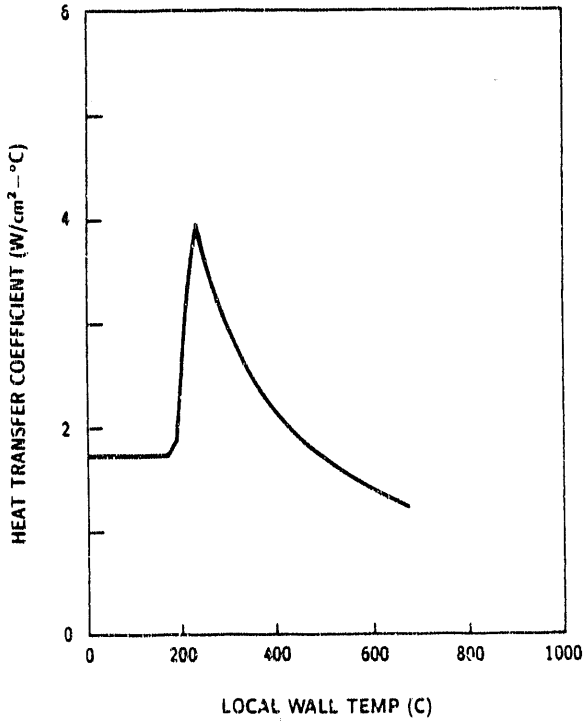

Fig. 2. Heat transfer coefficient for 6 mm channel (V = 4.0 m/s, P = 6.4 bar, TB = 37.0 C).

B. Finite Element Model

The finite element model for the TOPAZ2D code was of half a fin. The half fin was represented by 200 elements in the finite element mesh. The incident heat flux, the coolant bulk temperature and heat transfer coefficients calculated from the above procedure were the boundary conditions. The coolant temperature was set equal to the coolant temperature at the half-way length in the hypervapotron, where the experimental measurements were made. A steady-state calculation was performed. The aim was to calculate the temperature distribution in the hypervapotron and to compare the experimentally measured surface temperature with analysis.

IV. RESULTS

Figures 3 through 5 show the comparison of this analysis with experiments done at the JET Test Bed[2,3] on a shallow channel (3 mm channel) and deep channel (6 mm channel) hypervapotron. During the experiment, the inlet temperature of the coolant was 20°C. Hence, the bulk temperature of the coolant at the halfway length (where measurements and the analysis was performed) was different for each point on these plots. As seen in Fig. 3, the heat transfer has three regions. In region 1, the heat transfer is by forced convection. In region 2, part of the heat transfer surface reaches the incipient boiling temperature and therefore the heat transfer coefficient is higher than the forced convection region, thus the slope dT_s/dq'' is less than that for the pure forced-convection region. With further increase in heat transfer surface temperature, some of the surface reaches the critical heat flux condition described by Eq. (5), Thus, the heat transfer coefficient actually decreases with temperature beyond this point (Fig. 2). Due to this, the surface temperature rises rapidly with a heat flux increase (region 3). If it were not for the finned surface and large thermal conductivity of the copper, burn-out would have occurred at this time. Increasing the heat flux will ultimately make the local heat flux at all locations on the heat transfer surface greater than the critical heat flux region, and burn-out will occur.

Figures 3 through 5 show an excellent agreement between this analysis and the experimental results. This analysis covered a wide range of pressures, flow velocities and subcooling. It also covered two different geometries. In the future, an analysis will be performed to see if the model can predict performance of other geometries for which experimental data is available. An attempt could then be made to optimize the design of hypervapotrons for application to the ITER design.

Figures 6 through 8 show the isotherms in the hypervapotron for three flow regimes. Figure 6 is for a heat flux of 2 MW/m^2 and represents the forced convection regime because the temperatures over the entire heat transfer surface are below the incipient boiling temperature. As the surface heat flux is increased to 8 MW/m^2 (Fig. 7), part of the surface has nucleate boiling and part of the surface has forced convection. As the heat flux on the surface of the hypervapotron is increased to 25 MW/m^2, some part of the heat transfer surface reaches the critical heat flux condition (Fig. 8). However, burn-out is prevented due to conduction heat transfer to the colder surface. This is the important

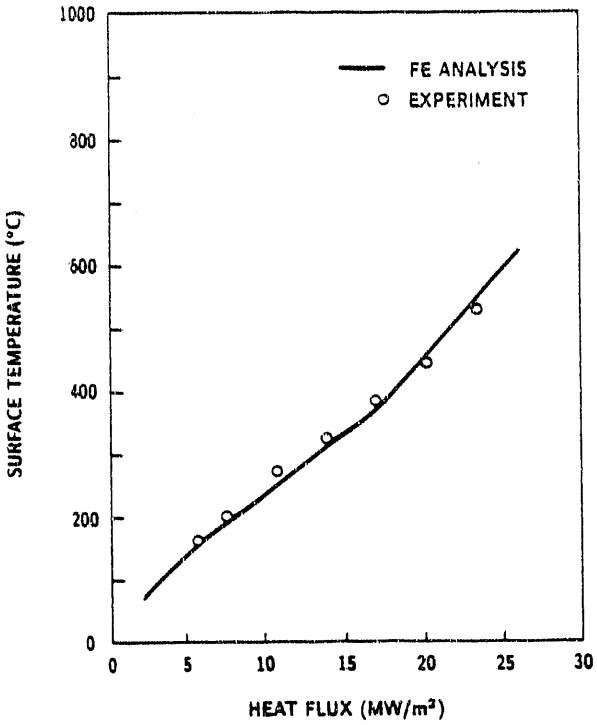

Fig. 3. Comparison of analysis and experiment for narrow channel vapotron, V = 8.4 m/s, P = 6.8 bar (inlet temperature of the coolant = 20°C).

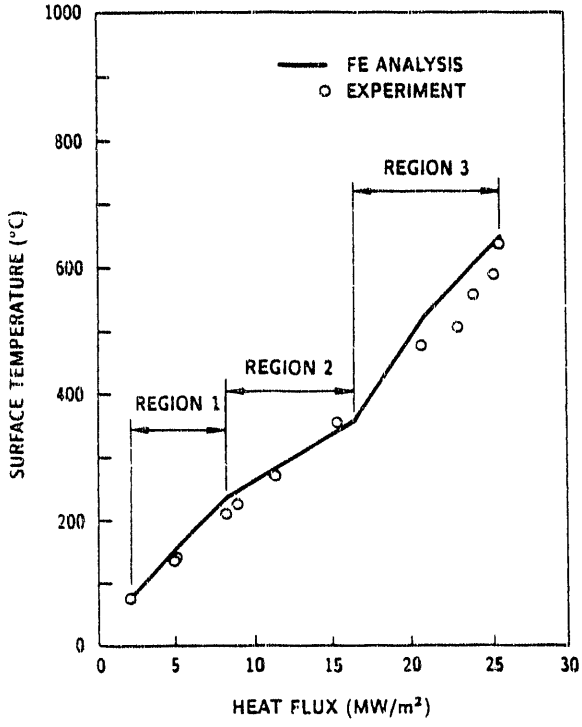

Fig. 4. Comparison of analysis and experiment for narrow channel vapotron, V = 11.5 m/s, P = 5.7 bar (inlet coolant temperature = 20°C).

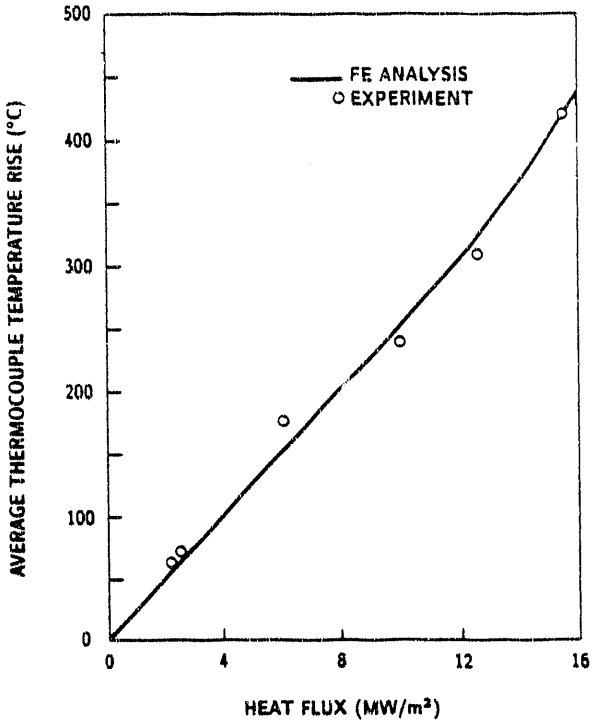

Fig. 5. Comparison of analysis and experiment for wide channel (6 mm) vapotron, V = 40 m/s, P = 6.4 bar (inlet coolant temperature = 20°C).

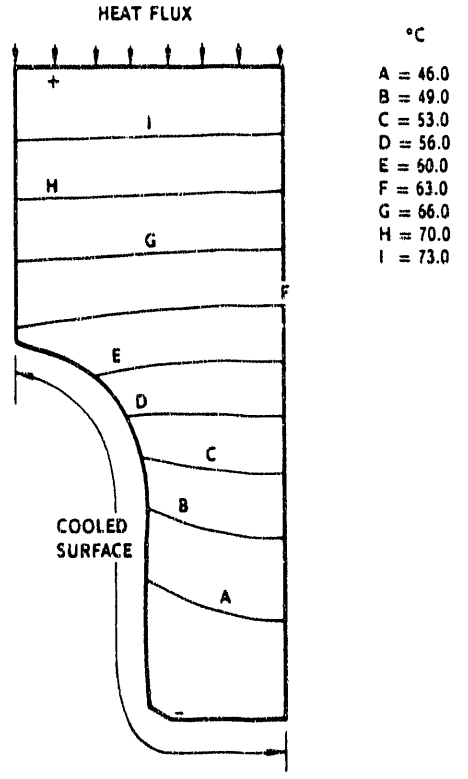

Fig. 6. Isotherms for forced convection regime (heat flux = 2 MW/m²).

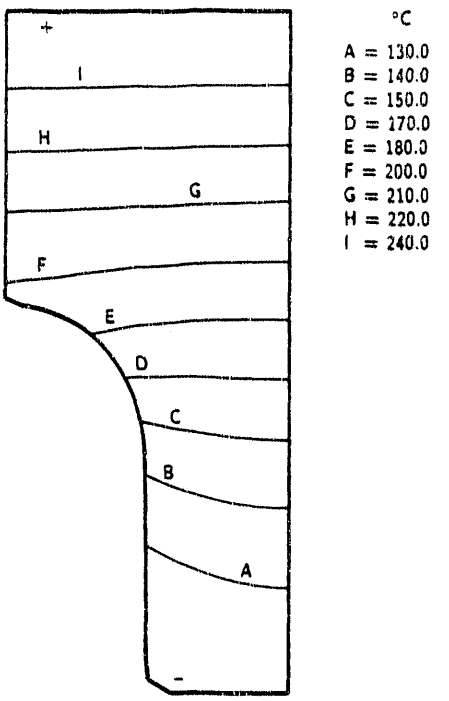

Fig. 7. Nucleate boiling regime (heat flux = 8 MW/m^2).

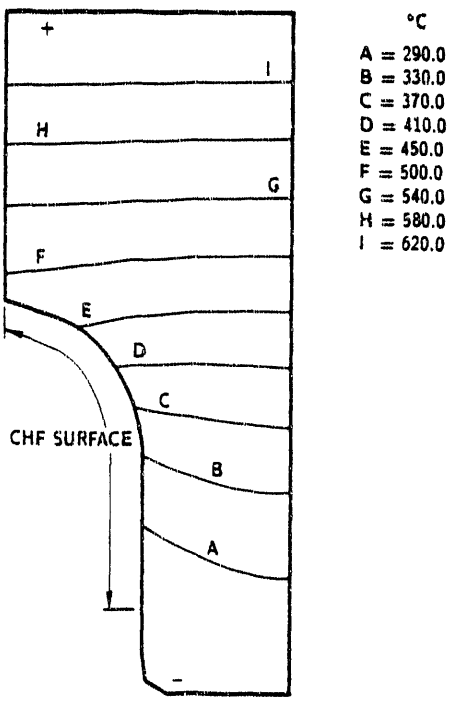

Fig. 8. Critical heat flux on large part of the heat transfer surface (heat flux = 25 MW/m^2).

feature of the hypervapotron where considerably higher heat flux on the surface than the critical heat flux in the coolant channel can be achieved.

The method presented above was used to analyze the performance of hypervapotron for materials other than copper. Figure 9 shows the effect of thermal conductivity on peak surface temperature at a surface heat flux of 25 MW/m^2. The result shows that the surface temperature for a hypervapotron made of materials other than copper will be considerably higher.

V. DISCUSSION

A method has been presented which predicts the thermal performance of a hypervapotron. Further work is planned to extend the method to a more general geometry. Two specific extensions of the method are anticipated: inclusion of three dimensional effects, and calculation of pressure oscillations during boiling.

VI. ACKNOWLEDGMENT

This is a report of work sponsored by the U.S. Department of Energy under Contract No. DE-AC03-89ER51114.

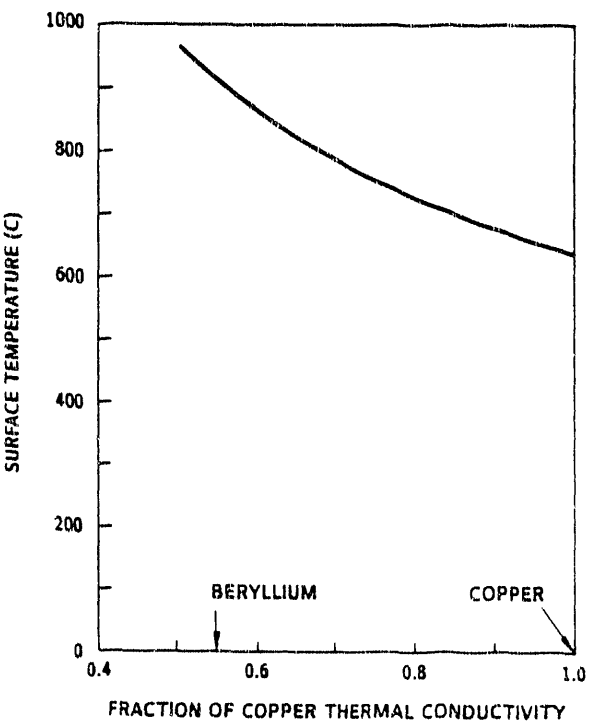

Fig. 9. Effect of thermal conductivity on surface temperature ($q'' = 25$ MW/m^2).

VII. REFERENCES

1. D. S. MILLER, "Internal Flow Systems," *BHRA Fluid Engineering* (1978).
2. H. FALTER et al., "Thermal Test Results of the JET Divertor Plate," *High Heat Flux Engineering* (SPIE Proceedings) Vol. 1739 (1992).
3. H. ALTMANN et al., "A Comparison Between Hypervapotron and Multitube High Heat Flux Stopping Elements," *Proc. SOFE*, Knoxville, 1989.
4. M. GREINER, "An Investigation of Resonant Heat Transfer Enhancement in Grooved Channels," *Int. J. Heat Mass Transfer*, **34**, 1383 (1991).
5. *Handbook of Heat Transfer Fundamentals* (W.M. ROSENOW et al., Eds.), McGraw-Hill Book Co., New York (1983).
6. A. E. BERGLES and W. M. ROSENOW, "The Determination of Forced Convection Surface Boiling Heat Transfer," paper 63-HT-22, presented at the Sixth National Heat Transfer Conference of the ASME-AIChE, Boston (1963).
7. J. R. S. THOM, W. M. WALKER, T. A. FALLON, and G. F. S. REISING, "Boiling in Subcooled Water During Flow in Tubes and Annuli," *Proc. Inst. Mech. Eng., (3C)*, **180** 226 (1965-1966).
8. A. E. BERGLES and W. M. ROSENOW, "The Determination of Forced Convection Surface Boiling Heat Transfer," *J. Heat Transfer*, **86**, 365 (1964).
9. J. G. COLLIER, *Convective Boiling and Condensation*, McGraw-Hill, New York (1972).
10. B. THOMPSON and R. V. MacBETH, "Boiling Water Heat Transfer — Burnout in Uniformly Heated Round Tubes: A Compilation of World Data with Accurate Correlations," AEEW-R, 356 (1964).
11. R. V. MacBETH, "Burn-out Analysis," Part 4, "Application of a Local Condition Hypothesis to World Data for Uniformly Heated Round Tubes and Rectangular Channels," AEEW-R, 267 (1963).
12. R. V. MacBETH, "Burn-out Analysis," Part 3, "The Low Velocity Burnout Regime," AEEW-R 222 (1963).
13. A. B. SHAPIRO, "TOPAZ — A Finite Element Heat Conduction Code," UCID-20045 (March 1984).

NOMENCLATURE

D	= hydraulic diameter of the flow channel without fins, m
ff	= factor, Eq. (1)
G	= mass flux, kg/m^2-sec
h	= heat transfer coefficient, W/m-°C
i	= enthalpy, kJ/kg
K	= thermal conductivity, W/m-°C
Nu	= Nusselt number = hD/K
p	= pressure, Pa
Pr	= Prandtl number
q''	= heat flux in cooling channel, MW/m^2
Q''	= incident heat flux, MW/m^2
Re	= Reynolds number
T	= temperature, °C
V	= velocity, m/sec
Z	= length, m
ΔT	= temperature difference, °C
Δi	= emthalpy difference, kJ/kg

Subscripts

b	= bulk
B	= boiling
Bi	= incipient boiling
CRIT	= critical
FC	= forced convection
ONB	= onset of boiling
SAT	= saturated
W	= wall

END

DATE FILMED

9/16/92